Article:
O'Hanlon, Simon J., Rieux, Adrien, Farrer, Rhys A. et al. (55 more authors) (2018) Recent Asian origin of chytrid fungi causing global amphibian declines. Science. pp. 621-627. ISSN: 0036-8075

https://doi.org/10.1126/science.aar1965

Title: Recent Asian origin of chytrid fungi causing global amphibian declines*

Authors: Simon J. O'Hanlon[1,2]*, Adrien Rieux[3], Rhys A. Farrer[1], Gonçalo M. Rosa[2,4,5], Bruce Waldman[6], Arnaud Bataille[6,7], Tiffany A. Kosch[8,6], Kris A. Murray[1], Balázs Brankovics[9,10], Matteo Fumagalli[11,31], Michael D. Martin[12,13], Nathan Wales[13], Mario Alvarado-Rybak[14], Kieran A. Bates[1,2], Lee Berger[8], Susanne Böll[15], Lola Brookes[2], Frances Clare[1,2], Elodie A. Courtois[16], Andrew A. Cunningham[2], Thomas M. Doherty-Bone[17], Pria Ghosh[1,18], David J. Gower[19], William E. Hintz[20], Jacob Höglund[21], Thomas S. Jenkinson[22], Chun-Fu Lin[23], Anssi Laurila[21], Adeline Loyau[24,25], An Martel[26], Sara Meurling[21], Claude Miaud[27], Pete Minting[28], Frank Pasmans[26], Dirk Schmeller[24,25], Benedikt R. Schmidt[29], Jennifer M. G. Shelton[1], Lee F. Skerratt[8], Freya Smith[2,30], Claudio Soto-Azat[14], Matteo Spagnoletti[31], Giulia Tessa[32], Luís Felipe Toledo[33], Andrés Valenzuela-Sánchez[34,14], Ruhan Verster[18], Judit Vörös[35], Rebecca J. Webb[8], Claudia Wierzbicki[1], Emma Wombwell[2], Kelly R. Zamudio[36], David M. Aanensen[37,1], Timothy Y. James[22], M. Thomas P. Gilbert[13,12], Ché Weldon[18], Jaime Bosch[38], François Balloux[31]†, Trenton W. J. Garner[2,18,32]†, Matthew C. Fisher[1]*

Affiliations:

[1] Department of Infectious Disease Epidemiology and MRC Centre for Global Infectious Disease Analysis, School of Public Health, Imperial College London, Norfolk Place, London W2 1PG, UK
[2] Institute of Zoology, Regent's Park, London, NW1 4RY, UK
[3] CIRAD, UMR PVBMT, 97410 St Pierre, Reunion, France[4] Department of Biology, University of Nevada, Reno, Reno NV 89557, USA
[5] Centre for Ecology, Evolution and Environmental Changes (CE3C), Faculdade de Ciências da Universidade de Lisboa, Lisboa, Portugal
[6] Laboratory of Behavioral and Population Ecology, School of Biological Sciences, Seoul National University, Seoul 08826, South Korea
[7] CIRAD, UMR ASTRE, F-34398 Montpellier, France
[8] One Health Research Group, College of Public Health, Medical and Veterinary Sciences, James Cook University, Townsville, Queensland, 4811, Australia
[9] Westerdijk Fungal Biodiversity Institute, Uppsalalaan 8, 3584CT Utrecht, The Netherlands
[10] Institute of Biodiversity and Ecosystem Dynamics, University of Amsterdam, Science Park 904, 1098 XH Amsterdam, The Netherlands
[11] Department of Life Sciences, Silwood Park Campus, Imperial College London, Ascot, UK
[12] Department of Natural History, NTNU University Museum, Norwegian University of Science and Technology (NTNU), Erling Skakkes gate 49, NO-7012 Trondheim, Norway
[13] Centre for GeoGenetics, Natural History Museum of Denmark, University of Copenhagen, Øster Voldgade 5-7, 1350 Copenhagen, Denmark
[14] Centro de Investigación para la Sustentabilidad, Facultad de Ecología y Recursos Naturales, Universidad Andres Bello, Republica 440, Santiago, Chile

[15] Agency for Population Ecology and Nature Conservancy, Gerbrunn
[16] Laboratoire Ecologie, évolution, interactions des systèmes amazoniens (LEEISA), Université de Guyane, CNRS, IFREMER, 97300 Cayenne, French Guiana.
[17] Conservation Programmes, Royal Zoological Society of Scotland, Edinburgh, UK
[18] Unit for Environmental Sciences and Management, Private Bag x6001, North-West University, Potchefstroom, 2520, South Africa
[19] Life Sciences, The Natural History Museum, London SW7 5BD, UK
[20] Biology Department, University of Victoria, Victoria, BC, V8W 3N5, Canada
[21] Department of Ecology and Genetics, EBC, Uppsala University. Norbyv. 18D, SE-75236, Uppsala, Sweden
[22] Department of Ecology and Evolutionary Biology, University of Michigan, Ann Arbor, MI, 48109, USA
[23] Zoology Division, Endemic Species Research Institute, 1 Ming-shen East Road, Jiji, Nantou 552, Taiwan
[24] Helmholtz Centre for Environmental Research – UFZ, Department of Conservation Biology, Permoserstrasse 15, 04318 Leipzig, Germany
[25] EcoLab, Université de Toulouse, CNRS, INPT, UPS, Toulouse, France
[26] Department of Pathology, Bacteriology and Avian Diseases, Faculty of Veterinary Medicine, Ghent University, Salisburylaan 133, B-9820 Merelbeke, Belgium
[27] PSL Research University, CEFE UMR 5175, CNRS, Université de Montpellier, Université Paul-Valéry Montpellier, EPHE, Montpellier, France
[28] Amphibian and Reptile Conservation (ARC) Trust, 655A Christchurch Road, Boscombe, Bournemouth, Dorset, UK, BH1 4AP
[29] Department of Evolutionary Biology and Environmental Studies, University of Zurich, Winterthurerstrasse 190, 8057 Zurich, Switzerland and Info Fauna Karch, UniMail - Bâtiment G, Bellevaux 51, 2000 Neuchâtel, Switzerland
[30] National Wildlife Management Centre, APHA, Woodchester Park, Gloucestershire GL10 3UJ, UK
[31] UCL Genetics Institute, University College London, Gower Street, WC1E 6BT, London, UK
[32] Non-profit Association Zirichiltaggi - Sardinia Wildlife Conservation, Strada Vicinale Filigheddu 62/C, I-07100 Sassari, Italy
[33] Laboratório de História Natural de Anfíbios Brasileiros (LaHNAB), Departamento de Biologia Animal, Instituto de Biologia, Unicamp, Campinas, Brazil
[34] ONG Ranita de Darwin, Nataniel Cox 152, Santiago, Chile
[35] Collection of Amphibians and Reptiles, Department of Zoology, Hungarian Natural History Museum, Budapest, Baross u. 13., 1088, Hungary
[36] Department of Ecology and Evolutionary Biology, Cornell University, Ithaca, NY, 14853, USA
[37] Centre for Genomic Pathogen Surveillance, Wellcome Genome Campus, Cambridgeshire, UK
[38] Museo Nacional de Ciencias Naturales, CSIC c/ Jose Gutierrez Abascal 2, 28006 Madrid, Spain

*Corresponding authors. Email: simon.ohanlon@gmail.com and matthew.fisher@imperial.ac.uk

†These authors share an equal contribution

89 **One Sentence Summary:** East Asia is the source of amphibian panzootic chytrid fungi
90 causing global amphibian declines that have emerged during the 20th century
91

Abstract:

Globalized infectious diseases are causing species declines worldwide but their source often remains elusive. We use whole-genome sequencing to solve the spatiotemporal origins of the most devastating panzootic to date, caused by the fungus *Batrachochytrium dendrobatidis*, a proximate driver of global amphibian declines. We trace the source of *B. dendrobatidis* to the Korean peninsula where one lineage, *Bd*ASIA-1, exhibits the genetic hallmarks of an ancestral population that seeded the panzootic. We date the emergence of this pathogen to the early 20th century coinciding with the global expansion of commercial trade in amphibians and show that intercontinental transmission is ongoing. Our findings point to East Asia as a geographic hotspot for *B. dendrobatidis* biodiversity, and the original source of these lineages that now parasitize amphibians worldwide.

Main Text:

Discovery of the amphibian-killing fungus *Batrachochytrium dendrobatidis* (*1, 2*) was a turning point in understanding why amphibian species worldwide are in steep decline. Amphibian declines and extinctions had been recorded by herpetologists as early as the 1970s, but were only recognized at a landmark meeting in 1990 as a global phenomenon which could not be explained by environmental changes and anthropogenic factors alone (*3*). The emergence of *B. dendrobatidis* and the disease that it causes, amphibian chytridiomycosis, as a causative agent of declines has been documented across six different regions: Australia (~1970s and 1990s) (*4*), Central America (~1970s) (*5*), South America (~1970s and 1980s) (*6, 7*), the Caribbean islands (~2000s) (*8*), the North American Sierra Nevada (~1980s and 1990s) (*9*), and the Iberian Peninsula (~1990s) (*10*). The panzootic has been attributed to the emergence of a single *B. dendrobatidis* lineage, known as *Bd*GPL (Global Panzootic Lineage) (*11*). However, twenty years after identification of the disease, the timing of its worldwide expansion remains unknown and previous estimates for time to most recent common ancestor (TMRCA) for *Bd*GPL span two orders of magnitude, from 100 ybp (*11*) to 26,000 ybp (*12*). The geographic origin of the pathogen is similarly contested, with the source of the disease variously suggested to be Africa (*13*), North America (*14*), South America (*15*), Japan (*16*) and East Asia (*17*).

Global diversity of *B. dendrobatidis*

To resolve these inconsistencies, we isolated *B. dendrobatidis* from all the candidate source continents and sequenced the genomes of 177 isolates to high depth then combined our data with published genomes from three prior studies (*11, 12, 18*) to generate a globally representative panel of 234 isolates (Fig. 1A). This dataset covers all continents from which *B. dendrobatidis* has been detected to date, and spans infections of all three extant orders of

Amphibia (Fig. S1 and Table S1). Mapped against the *B. dendrobatidis* reference genome JEL423, our sequencing recovered 586,005 segregating single nucleotide polymorphisms (SNPs). Phylogenetic analysis recovered all previously detected divergent lineages (Fig. 1B and Fig. S2). The previously accepted lineages *Bd*GPL (global), *Bd*CAPE (African), *Bd*CH (European) and *Bd*BRAZIL (Brazilian), were all detected (*19*), but our discovery of a new hyperdiverse lineage in amphibians native to the Korean peninsula (*Bd*ASIA-1) redefined these lineages and their relationships. The *Bd*CH lineage, which was previously thought to be enzootic to Switzerland (*11*) now groups with the *Bd*ASIA-1 lineage. A second Asian-associated lineage (*Bd*ASIA-2) was recovered from invasive North American bullfrogs in Korea and is closely related to the lineage that is enzootic to the Brazilian Atlantic forest (*Bd*BRAZIL) (*20*). It was not possible to infer the direction of intercontinental spread between isolates within this lineage so it was named *Bd*ASIA-2/*Bd*BRAZIL. Conditional on the midpoint rooting of the phylogeny in Fig. 1B, we now define the main diverged lineages as *Bd*GPL, *Bd*CAPE, *Bd*ASIA-1 (which includes the single *Bd*CH isolate) and *Bd*ASIA-2/*Bd*BRAZIL. Previous phylogenetic relationships developed using the widely used ribosomal intragenic spacer *ITS-1* region do not accurately distinguish *B. dendrobatidis* lineages (Fig. S3) and this likely explains much of the place-of-origin conflict in the literature (*15-17*).

Pairwise comparisons among isolates within each lineage show that the average number of segregating sites is three-fold greater for *Bd*ASIA-1 than for any other lineage (Fig. 1A and Table 1) and that nucleotide diversity (π; Fig. S4) is two to four-fold greater. Seven of our eight *Bd*ASIA-1 isolates were recently cultured from wild South Korean frogs while the other came from the pet-trade in Belgium, all of which were aclinical infections. These isolates show that the Korean peninsula is a global centre of *B. dendrobatidis* diversity and that East Asia may contain the ancestral population of *B. dendrobatidis*, as suggested by Bataille *et al*

(*17*). We investigated this hypothesis further using Bayesian-based haplotype clustering (*21*) and found the greatest haplotype sharing among isolates within *Bd*ASIA-1 and between *Bd*ASIA-1 and all other lineages. This provides direct genetic evidence that *Bd*ASIA-1 shares more diversity with the global population of *B. dendrobatidis* than any other lineage (Fig. S5). In an independent test of ancestry, we used OrthoMCL (*22*) to root a *B. dendrobatidis* phylogeny to its closest known relative *B. salamandrivorans* which currently threatens salamanders (*23*). This tree indicates that the Asian and Brazilian isolates of *B. dendrobatidis* lie outside a clade comprising all other isolates (Fig. S6 and Table S2). To identify the signature of demographic histories across lineages we used Tajima's *D* (*24*). Genome scans of most lineages showed highly variable positive and negative values of *D* with maxima exhibited by *Bd*GPL (-2.6 to +6.2; Fig. 2F), indicating that these lineages (*Bd*ASIA-2/*Bd*BRAZIL, *Bd*CAPE and *Bd*GPL) have undergone episodes of population fluctuation, strong natural selection, or both, that are consistent with a history of spatial and host radiations. In striking contrast, *Bd*ASIA-1 shows a flat profile for Tajima's *D* (Fig. 2F) indicating mutation-drift equilibrium likely reflective of pathogen endemism in this region.

Dating the emergence of *Bd*GPL

The broad range of previous estimates for the TMRCA of *Bd*GPL spanning 26,000 years (*11, 12*) can be explained by two sources of inaccuracy: (1) unaccounted recombination and (2) the application of unrealistic evolutionary rates. To address these, we first interrogated the 178,280 kbp mitochondrial genome (mtDNA), which has high copy number and low rates of recombination compared to the nuclear genome. To resolve the structure of the mtDNA genome we resorted to long-read sequencing using a MinION device (Oxford Nanopore Technologies, Cambridge, UK), which allowed us to describe this molecules unusual configuration; *Batrachochytrium dendrobatidis* carries three linear mitochondrial segments, each having inverted repeats at the termini with conserved mitochondrial genes spread over

two of the segments (Fig. S7). Additionally, we sought regions of the autosomal genome with low rates of recombination to obtain an independent estimate of the TMRCA of *Bd*GPL.

Detection of crossover events in the *B. dendrobatidis* autosomal genome (*18*) using a subset of the isolates in this study revealed a large (1.66Mbp) region of Supercontig_1.2 in *Bd*GPL that exhibits several features that identified it as a recombination 'coldspot': (1) a continuous region of reduced Tajima's *D* (Fig. 2D); (2) sustained high values of F_{ST} when compared with all other lineages (Fig. 3A); (3) a continuous region of reduced nucleotide diversity (π, Fig. S4) and (4) shared loss-of-heterozygosity (Fig. S8). We expanded sampling to infer the temporal range of pathogen introductions using a broad panel of isolates with known date of isolation (n = 184, ranging from 1998 to 2016) and whole-genome RNA-baiting to obtain reads from preserved amphibians that had died of chytridiomycosis. We then investigated whether our dataset contained sufficient signal to perform tip-dating inferences by building phylogenetic trees using PhyML (*25*) (Fig. 2A and 2C) then fitting root-to-tip distances to collection dates both at the whole-tree and within-lineage scales. We observed a positive and significant correlation within *Bd*GPL only, for both the mitochondrial and nuclear genomes, demonstrating sufficient temporal signal to perform thorough tip-dating inferences at this evolutionary scale (Fig. 2B and 2D).

Tip-dating in BEAST was used to co-estimate ancestral divergence times and the rate at which mutations accumulate within the *Bd*GPL lineage. The mean mitochondrial substitution rate was 1.01×10^{-6} substitutions/site/year (95% highest posterior density (HPD) 4.29×10^{-7} – 1.62×10^{-6}). The mean nuclear substitution rate was 7.29×10^{-7} substitutions/site/year (95% HPD 3.41×10^{-7} – 1.14×10^{-6}), which is comparable to a recent report of an evolutionary rate of $2.4 – 2.6 \times 10^{-6}$ substitutions/site/year for another unicellular yeast, *Saccharomyces cerevisiae* beer strains (*26*). These estimates are over 300-fold faster than the rate used in a

previous study (*12*) to obtain a TMRCA of 26,400 years for *Bd*GPL. Accordingly, we estimate the ancestor of the amphibian panzootic *Bd*GPL originated between 120 and 50 years ago (Fig. 2E), with HPD estimates of 1898 [95% HPD 1809-1941] and 1962 [95% HPD 1859-1988] for the nuclear and mitochondrial dating analyses respectively (Fig. 2F).

We considered an additional calibration approach for the TMRCA of the mitochondrial genome where we included informative priors on nodes around the dates for the first historical descriptions of *Bd*GPL detection in Australia (1978), Central America (1972), Sierra de Guadarrama (Europe) (1997), and the Pyrenees (Europe) (2000). We did not include priors for nodes where observed declines have been reported, but where the lineage responsible for those declines is unknown. This mixed dating method based on tips and nodes calibration yielded very similar estimates (TMRCA estimates of 1975 [95% HPD 1939 – 1989] (Fig. S9)), further strengthening our confidence in a recent date of emergence for *Bd*GPL. An expansion of *Bd*GPL in the 20th century coincides with the global expansion in amphibians traded for exotic pets, medical and food purposes (*27, 28*). Within our phylogeny, we found representatives from all lineages among traded animals (Figs. S10-14), and identified ten events where traded amphibians were infected with non-enzootic isolates (Fig. 4). This finding demonstrates the ongoing failure of international biosecurity despite the listing of *B. dendrobatidis* by the World Organisation for Animal Health (the OIE) in 2008.

Hybridisation between recontacting lineages of *B. dendrobatidis*

To determine the extent to which the four main lineages of *B. dendrobatidis* have undergone recent genetic exchange, we used the site-by-site based approach implemented in STRUCTURE (*29*). Although most isolates could be assigned unambiguously to one of the four main lineages, we identified three hybrid genotypes (Fig. 3B), including one previously reported hybrid (isolate CLFT024/2) (*20*), and discovered two newly identified hybrids of

*Bd*GPL and *Bd*CAPE in South Africa. Furthermore, *Bd*CH (isolate 0739) appears to be a chimera of multiple lineages that may represent unsampled genomic diversity that resides in East Asia, rather than true hybridisation. These hybrid genomes demonstrate that *B. dendrobatidis* is continuing to exchange haplotypes among lineages when they interact following continental invasions, generating novel genomic diversity. We analysed isolate clustering using principle components analysis on a filtered subset of 3,900 SNPs in linkage equilibrium, revealing an overall population structure that is consistent with our phylogenetic analyses (Fig 3C). In addition, the putatively identified hybrid isolates of *B. dendrobatidis* were shown to fall between main lineage clusters (Fig. 3C) further strengthening our hypothesis of haplotype exchange occurring during secondary contact between lineages.

Associations among lineage, virulence and declines

Genotypic diversification of pathogens is commonly associated with diversification of traits associated with host exploitation (*30*), and is most commonly measured as the ability to infect a host and to cause disease post-infection. We tested for variation of these two phenotypic traits across four *B. dendrobatidis* lineages by exposing larval and post-metamorphic common toads (*Bufo bufo*). Larvae are highly susceptible to infection but do not die before metamorphosis, in contrast to post-metamorphic juveniles, which are susceptible to infection and fatal chytridiomycosis (*31*). In tadpoles, both *Bd*GPL and *Bd*ASIA-1 were significantly more infectious than *Bd*CAPE and *Bd*CH (Fig. S15 and Tables S3 & S4). In metamorphs, *Bd*GPL was significantly more infectious than the other treatments, compared to the control group, and significantly more lethal in experimental challenge, than the geographically more restricted *Bd*CAPE, *Bd*ASIA-1 and *Bd*CH (Fig. 2G). We further tested for differences in virulence among lineages by using our global dataset to examine whether chytridiomycosis was non-randomly associated with *B. dendrobatidis* lineage. We detected a significant

difference ($p < 0.001$) in the proportion of isolates associated with chytridiomycosis among the three parental lineages (*Bd*ASIA-1 and *Bd*ASIA-2/*Bd*BRAZIL were grouped due to low sample sizes), and *post hoc* tests indicated significant excess in virulence in both *Bd*GPL and *Bd*CAPE lineages relative to the combined *Bd*ASIA-1 and *Bd*ASIA-2/*Bd*BRAZIL (all $p < 0.05$). However, we did not detect a significant difference between *Bd*GPL and *Bd*CAPE (Fig. S16 and Table S5). These data suggest that although *Bd*GPL is highly virulent, population-level outcomes are also context dependent (*32*); under some conditions other lineages can also be responsible for lethal amphibian disease and population declines (*33*).

Historical and contemporary implications of panzootic chytridiomycosis

Our results point to endemism of *B. dendrobatidis* in Asia, out of which multiple panzootic lineages have emerged. These emergent diasporas include the virulent and highly transmissible *Bd*GPL which spread during the early 20th century via a yet unknown route to infect close to 700 amphibian species out of ~1300 thus far tested (*34*). With over 7800 amphibian species currently described, the number of affected species is likely to rise. The international trade in amphibians has undoubtedly contributed directly to vectoring this pathogen worldwide (Fig. 4; *35,36*), and within our phylogeny we identified many highly supported (≥ 90% bootstrap support) clades on short branches that linked isolates collected from wild amphibian populations across different continents (Fig. 4; Fig. S10-S14). However, the role of globalised trade in passively contributing to the spread of this disease cannot be ruled out. It is likely no coincidence that our estimated dates for the emergence of *Bd*GPL span the globalisation 'big bang', the rapid proliferation in intercontinental trade, capital, and technology that started in the 1820s (*37*). The recent invasion of Madagascar by Asian common toads hidden within mining equipment (*38*) demonstrates the capacity for amphibians to escape detection at borders and exemplifies how the unintended anthropogenic

dispersal of amphibians has also likely contributed to the worldwide spread of pathogenic chytrids.

The hyperdiverse hotspot identified in Korea likely represents a fraction of the *Batrachochytrium* genetic diversity in Asia and further sampling across this region is urgently needed because the substantial global trade in Asian amphibians (*39*) presents a risk of seeding future outbreak lineages. Unique ribosomal DNA haplotypes of *B. dendrobatidis* have been detected in native amphibian species in India (*40, 41*), Japan (*16*) and China (*42*). Although caution should be observed when drawing conclusions about lineages based on short sequence alignments (Fig. S3), other endemic lineages probably remain undetected within Asia. Significantly, the northern European countryside is witnessing the emergence of *B. salamandrivorans*, which also has its origin in Asia. The emergence of *B. salamandrivorans* is linked to the amphibian pet trade (*43*), and the broad expansion of virulence factors that are found in the genomes of these two pathogens are testament to the evolutionary innovation that has occurred in these Asian *Batrachochytrium* fungi (*23*). Our findings show that the global trade in amphibians continues to be associated with the translocation of chytrid lineages with panzootic potential. Ultimately, our work confirms that panzootics of emerging fungal diseases in amphibians are caused by ancient patterns of pathogen phylogeography being redrawn as largely unrestricted global trade moves pathogens into new regions, infecting new hosts and igniting disease outbreaks. Within this context, the continued strengthening of transcontinental biosecurity is critical to the survival of amphibian species in the wild (*44*).

References:

1. M. C. Fisher, D. A. Henk, C. J. Briggs, J. S. Brownstein, L. C. Madoff, S. L. McCraw, S. J. Gurr, Emerging fungal threats to animal, plant and ecosystem health. *Nature* **484**, 186-194 (2012).
2. L. Berger, R. Speare, P. Daszak, D. E. Green, A. A. Cunningham, C. L. Goggin, R. Slocombe, M. A. Ragan, A. H. Hyatt, K. R. McDonald, H. B. Hines, K. R. Lips, G. Marantelli, H. Parkes, Chytridiomycosis causes amphibian mortality associated with population declines in the rain forests of Australia and Central America. *P Natl Acad Sci USA* **95**, 9031-9036 (1998).
3. A. R. Blaustein, D. B. Wake, Declining amphibian populations: A global phenomenon? *Trends Ecol Evol* **5**, 203-204 (1990).
4. L. F. Skerratt, L. Berger, R. Speare, S. Cashins, K. R. McDonald, A. D. Phillott, H. B. Hines, N. Kenyon, Spread of chytridiomycosis has caused the rapid global decline and extinction of frogs. *Ecohealth* **4**, 125-134 (2007).
5. T. L. Cheng, S. M. Rovito, D. B. Wake, V. T. Vredenburg, Coincident mass extirpation of neotropical amphibians with the emergence of the infectious fungal pathogen *Batrachochytrium dendrobatidis*. *P Natl Acad Sci USA* **108**, 9502-9507 (2011).
6. K. R. Lips, J. Diffendorfer, J. R. Mendelson, M. W. Sears, Riding the wave: Reconciling the roles of disease and climate change in amphibian declines. *Plos Biol* **6**, 441-454 (2008).
7. T. Carvalho, C. G. Becker, L. F. Toledo, Historical amphibian declines and extinctions in Brazil linked to chytridiomycosis. *Proc Royal Soc B* **284**, 20162254 (2017).
8. M. A. Hudson, R. P. Young, J. D. Jackson, P. Orozco-terWengel, L. Martin, A. James, M. Sulton, G. Garcia, R. A. Griffiths, R. Thomas, C. Magin, M. W. Bruford, A. A. Cunningham, Dynamics and genetics of a disease-driven species decline to near extinction: lessons for conservation. *Sci Rep* **6**, srep30772 (2016).

9. L. J. Rachowicz, R. A. Knapp, J. A. T. Morgan, M. J. Stice, V. T. Vredenburg, J. M. Parker, C. J. Briggs, Emerging infectious disease as a proximate cause of amphibian mass mortality. *Ecology* **87**, 1671-1683 (2006).

10. J. Bosch, I. Martinez-Solano, M. Garcia-Paris, Evidence of a chytrid fungus infection involved in the decline of the common midwife toad (*Alytes obstetricans*) in protected areas of central Spain. *Biol Conserv* **97**, 331-337 (2001).

11. R. A. Farrer, L. A. Weinert, J. Bielby, T. W. J. Garner, F. Balloux, F. Clare, J. Bosch, A. A. Cunningham, C. Weldon, L. H. du Preez, L. Anderson, S. L. K. Pond, R. Shahar-Golan, D. A. Henk, M. C. Fisher, Multiple emergences of genetically diverse amphibian-infecting chytrids include a globalized hypervirulent recombinant lineage. *P Natl Acad Sci USA* **108**, 18732-18736 (2011).

12. E. B. Rosenblum, T. Y. James, K. R. Zamudio, T. J. Poorten, D. Ilut, D. Rodriguez, J. M. Eastman, K. Richards-Hrdlicka, S. Joneson, T. S. Jenkinson, J. E. Longcore, G. P. Olea, L. F. Toledo, M. L. Arellano, E. M. Medina, S. Restrepo, S. V. Flechas, L. Berger, C. J. Briggs, J. E. Stajich, Complex history of the amphibian-killing chytrid fungus revealed with genome resequencing data. *P Natl Acad Sci USA* **110**, 9385-9390 (2013).

13. C. Weldon, L. H. du Preez, A. D. Hyatt, R. Muller, R. Speare, Origin of the amphibian chytrid fungus. *Emerg Infect Dis* **10**, 2100-2105 (2004).

14. B. L. Talley, C. R. Muletz, V. T. Vredenburg, R. C. Fleischer, K. R. Lips, A century of *Batrachochytrium dendrobatidis* in Illinois amphibians (1888-1989). *Biol Conserv* **182**, 254-261 (2015).

15. D. Rodriguez, C. G. Becker, N. C. Pupin, C. F. B. Haddad, K. R. Zamudio, Long-term endemism of two highly divergent lineages of the amphibian-killing fungus in the Atlantic Forest of Brazil. *Mol Ecol* **23**, 774-787 (2014).

16. K. Goka, J. Yokoyama, Y. Une, T. Kuroki, K. Suzuki, M. Nakahara, A. Kobayashi, S. Inaba, T. Mizutani, A. D. Hyatt, Amphibian chytridiomycosis in Japan: distribution, haplotypes and possible route of entry into Japan. *Mol Ecol* **18**, 4757-4774 (2009).

17. A. Bataille, J. J. Fong, M. Cha, G. O. U. Wogan, H. J. Baek, H. Lee, M. S. Min, B. Waldman, Genetic evidence for a high diversity and wide distribution of endemic strains of the pathogenic chytrid fungus *Batrachochytrium dendrobatidis* in wild Asian amphibians. *Mol Ecol* **22**, 4196-4209 (2013).

18. R. A. Farrer, D. A. Henk, T. W. J. Garner, F. Balloux, D. C. Woodhams, M. C. Fisher, Chromosomal copy number variation, selection and uneven rates of recombination reveal cryptic genome diversity linked to pathogenicity. *Plos Genet* **9**, e1003703 (2013).

19. S. Argimón, K. Abudahab, R. J. E. Goater, A. Fedosejev, J. Bhai, C. Glasner, E. J. Feil, M. T. G. Holden, C. A. Yeats, H. Grundmann, B. G. Spratt, D. M. Aanensen, Microreact: visualizing and sharing data for genomic epidemiology and phylogeography. Microbial Genomics **2**, e000093 (2016).

20. L. M. Schloegel, L. F. Toledo, J. E. Longcore, S. E. Greenspan, C. A. Vieira, M. Lee, S. Zhao, C. Wangen, C. M. Ferreira, M. Hipolito, A. J. Davies, C. A. Cuomo, P. Daszak, T. Y. James, Novel, panzootic and hybrid genotypes of amphibian chytridiomycosis associated with the bullfrog trade. *Mol Ecol* **21**, 5162-5177 (2012).

21. D. J. Lawson, G. Hellenthal, S. Myers, D. Falush, Inference of population structure using dense haplotype data. *Plos Genet* **8**, e1002453 (2012).

22. L. Li, C. J. Stoeckert, Jr., D. S. Roos, OrthoMCL: identification of ortholog groups for eukaryotic genomes. *Genome Res* **13**, 2178-2189 (2003).

23. R. A. Farrer, A. Martel, E. Verbrugghe, A. Abouelleil, R. Ducatelle, J. E. Longcore, T. Y. James, F. Pasmans, M. C. Fisher, C. A. Cuomo, Genomic innovations linked to infection strategies across emerging pathogenic chytrid fungi. *Nat Commun* **8**, 14742 (2017).

24. F. Tajima, Statistical-Method for Testing the Neutral Mutation Hypothesis by DNA Polymorphism. *Genetics* **123**, 585-595 (1989).

25. S. Guindon, J. F. Dufayard, V. Lefort, M. Anisimova, W. Hordijk, O. Gascuel, New algorithms and methods to estimate maximum-likelihood phylogenies: assessing the performance of PhyML 3.0. *Syst Biol* **59**, 307-321 (2010).

26. B. Gallone, J. Steensels, T. Prahl, L. Soriaga, V. Saels, B. Herrera-Malaver, A. Merlevede, M. Roncoroni, K. Voordeckers, L. Miraglia, C. Teiling, B. Steffy, M. Taylor, A. Schwartz, T. Richardson, C. White, G. Baele, S. Maere, K. J. Verstrepen, Domestication and divergence of *Saccharomyces cerevisiae* beer yeasts. *Cell* **166**, 1397-1410.e16 (2016).

27. M. C. Fisher, T. W. J. Garner, The relationship between the emergence of *Batrachochytrium dendrobatidis*, the international trade in amphibians and introduced amphibian species. *Fungal Biol Rev* **21**, 2-9 (2007).

28. A. I. Carpenter, F. Andreone, R. D. Moore, R. A. Griffiths, A review of the international trade in amphibians: the types, levels and dynamics of trade in CITES-listed species. *Oryx* **48**, 565-574 (2014).

29. J. K. Pritchard, M. Stephens, P. Donnelly, Inference of population structure using multilocus genotype data. *Genetics* **155**, 945-959 (2000).

30. S. J. Price, T. W. Garner, R. A. Nichols, F. Balloux, C. Ayres, A. Mora-Cabello de Alba, J. Bosch, Collapse of amphibian communities due to an introduced ranavirus. *Curr Biol* **24**, 2586-2591 (2014).

31. T. W. J. Garner, S. Walker, J. Bosch, S. Leech, J. M. Rowcliffe, A. A. Cunningham, M. C. Fisher, Life history tradeoffs influence mortality associated with the amphibian pathogen *Batrachochytrium dendrobatidis. Oikos* **118**, 783-791 (2009).

32. K. A. Bates, F. C. Clare, S. O'Hanlon, J. Bosch, L. Brookes, K. Hopkins, E. J. McLaughlin, O. Daniel, T. W. J. Garner, M. C. Fisher, X. A. Harrison, Amphibian chytridiomycosis outbreak dynamics are linked with host skin bacterial community structure. *Nat Commun* **9**, 693 (2018).

33. B. J. Doddington, J. Bosch, J. A. Oliver, N. C. Grassly, G. Garcia, B. R. Schmidt, T. W. Garner, M. C. Fisher, Context-dependent amphibian host population response to an invading pathogen. *Ecology* **94**, 1795-1804 (2013).

34. D. H. Olson, K. L. Ronnenberg, Global Bd Mapping Project: 2014 Update. FrogLog. 22, p17-21 (2014).

35. S. F. Walker, J. Bosch, T. Y. James, A. P. Litvintseva, J. A. O. Valls, S. Piña, G. García, G. A. Rosa, A. A. Cunningham, S. Hole, R. Griffiths, M. C. Fisher, Invasive pathogens threaten species recovery programs, *Curr Biol* **18**, R853-R854 (2008).

36. E. L. Wombwell, T. W. J. Garner, A. A. Cunningham, R. Quest, S. Pritchard, J. M. Rowcliffe, R. Griffiths, Detection of *Batrachochytrium dendrobatidis* in amphibians imported into the UK for the pet trade. *EcoHealth* **13**, 456-466 (2016).

37. K. H. O'Rourke, J. G. Williamson, When did globalisation begin? *Eur Rev Econ Hist* **6**, 23–50 (2002).

38. J. E. Kolby, Ecology: Stop Madagascar's toad invasion now, *Nature* **509**, 563 (2014).

39. A. Herrel, A. van der Meijden, An analysis of the live reptile and amphibian trade in the USA compared to the global trade in endangered species. *Herpetol J* **24**, 103-110 (2014).

40. N. Dahanukar, K. Krutha, M. S. Paingankar, A. D. Padhye, N. Modak, S. Molur, Endemic Asian chytrid strain infection in threatened and endemic anurans of the northern Western Ghats, India. *PLoS One* **8**, e77528 (2013)

41. S. Molur, K. Krutha, M.S. Paingankar, N. Dahanukar, Asian strain of *Batrachochytrium dendrobatidis* is widespread in the Western Ghats, India. *Dis Aquat Organ* **112**, 251-255 (2015).

42. C. Bai, X. Liu, M. C. Fisher, W. J. T. Garner, Y. Li, Global and endemic Asian lineages of the emerging pathogenic fungus *Batrachochytrium dendrobatidis* widely infect amphibians in China. *Divers Distrib* **18**, 307-318 (2012).

43. A. Martel, M. Blooi, C. Adriaensen, P. Van Rooij, W. Beukema, M. C. Fisher, R. A. Farrer, B. R. Schmidt, U. Tobler, K. Goka, K. R. Lips, C. Muletz, K. R. Zamudio, J. Bosch, S. Lotters, E. Wombwell, T. W. Garner, A. A. Cunningham, A. Spitzen-van der Sluijs, S. Salvidio, R. Ducatelle, K. Nishikawa, T. T. Nguyen, J. E. Kolby, I. Van Bocxlaer, F. Bossuyt, F. Pasmans, Wildlife disease. Recent introduction of a chytrid fungus endangers Western Palearctic salamanders. *Science* **346**, 630-631 (2014).

44. H. E. Roy, H. Hesketh, B. V. Purse, J. Eilenberg, A. Santini, R. Scalera, G. D. Stentiford, T. Adriaens, K. Bacela-Spychalska, D. Bass, K. M. Beckmann, P. Bessell, J. Bojko, O. Booy, A.

C. Cardoso, F. Essl, Q. Groom, C. Harrower, R. Kleespies, A. F. Martinou, M. M. van Oers, E. J. Peeler, J. Pergl, W. Rabitsch, A. Roques, F. Schaffner, S. Schindler, B. R. Schmidt, K. Schonrogge, J. Smith, W. Solarz, A. Stewart, A. Stroo, E. Tricarico, K. M. A. Turvey, A. Vannini, M. Vila, S. Woodward, A. A. Wynns, A. M. Dunn, Alien pathogens on the horizon: opportunities for predicting their threat to wildlife. *Conserv Lett* **10**, 477-484 (2017).

45. M. Martin, Cutadapt removes adapter sequences from high-throughput sequencing reads. *EMBnet. journal* **17**, 10-12 (2011).

46. H. Li, Aligning sequence reads, clone sequences and assembly contigs with BWA-MEM. *arXiv preprint arXiv:1303.3997*, (2013).

47. H. Li, B. Handsaker, A. Wysoker, T. Fennell, J. Ruan, N. Homer, G. Marth, G. Abecasis, R. Durbin, The sequence alignment/map format and SAMtools. *Bioinformatics* **25**, 2078-2079 (2009).

48. E. Garrison, G. Marth, Haplotype-based variant detection from short-read sequencing. *arXiv preprint arXiv:1207.3907*, (2012).

49. E. Garrison, Vcflib: A C++ library for parsing and manipulating VCF files. *GitHub* https://github/. *com/ekg/vcflib (accessed July 21, 2015)*, (2012).

50. A. Tan, G. R. Abecasis, H. M. Kang, Unified representation of genetic variants. *Bioinformatics* **31**, 2202-2204 (2015).

51. A. Stamatakis, RAxML version 8: a tool for phylogenetic analysis and post-analysis of large phylogenies. *Bioinformatics* **30**, 1312-1313 (2014).

52. A. McKenna, M. Hanna, E. Banks, A. Sivachenko, K. Cibulskis, A. Kernytsky, K. Garimella, D. Altshuler, S. Gabriel, M. Daly, The Genome Analysis Toolkit: a MapReduce framework for analyzing next-generation DNA sequencing data. *Genome Res* **20**, 1297-1303 (2010).

53. S. Guindon, J. F. Dufayard, V. Lefort, M. Anisimova, W. Hordijk, O. Gascuel, New algorithms and methods to estimate maximum-likelihood phylogenies: assessing the performance of PhyML 3.0. *Syst Biol* **59**, 307-321 (2010).

54. A. J. Drummond, M. A. Suchard, D. Xie, A. Rambaut, Bayesian phylogenetics with BEAUti and the BEAST 1.7. *Mol Biol Evol* **29**, 1969-1973 (2012).

55. D. Posada, K. A. Crandall, MODELTEST: testing the model of DNA substitution. *Bioinformatics* **14**, 817-818 (1998).

56. A. Rieux, F. Balloux, Inferences from tip-calibrated phylogenies: a review and a practical guide. *Mol Ecol*, **25**, 1911-1924 (2016).

57. S. F. Walker, J. Bosch, V. Gomez, T. W. Garner, A. A. Cunningham, D. S. Schmeller, M. Ninyerola, D. A. Henk, C. Ginestet, C. P. Arthur, M. C. Fisher, Factors driving pathogenicity vs. prevalence of amphibian panzootic chytridiomycosis in Iberia. *Ecol Lett* **13**, 372-382 (2010).

58. N. Wales, C. Caroe, M. Sandoval-Velasco, C. Gamba, R. Barnett, J. A. Samaniego, J. R. Madrigal, L. Orlando, M. T. Gilbert, New insights on single-stranded versus double-stranded DNA library preparation for ancient DNA. *BioTechniques* **59**, 368-371 (2015).

59. M. Schubert, L. Ermini, C. Der Sarkissian, H. Jonsson, A. Ginolhac, R. Schaefer, M. D. Martin, R. Fernandez, M. Kircher, M. McCue, E. Willerslev, L. Orlando, Characterization of ancient and modern genomes by SNP detection and phylogenomic and metagenomic analysis using PALEOMIX. *Nat Protoc* **9**, 1056-1082 (2014).

60. S. Koren, B. P. Walenz, K. Berlin, J. R. Miller, N. H. Bergman, A. M. Phillippy, Canu: scalable and accurate long-read assembly via adaptive k-mer weighting and repeat separation. *Genome Res* **27**, 722-736 (2017).

61. I. Sovic, M. Sikic, A. Wilm, S. N. Fenlon, S. Chen, N. Nagarajan, Fast and sensitive mapping of nanopore sequencing reads with GraphMap. *Nat Commun* **7**, 11307 (2016).

62. B. J. Walker, T. Abeel, T. Shea, M. Priest, A. Abouelliel, S. Sakthikumar, C. A. Cuomo, Q. Zeng, J. Wortman, S. K. Young, A. M. Earl, Pilon: an integrated tool for comprehensive microbial variant detection and genome assembly improvement. *PLoS One* **9**, e112963 (2014).

63. N. Beck, B. Lang, MFannot. *MFannot Tool* Available at: http://megasun.bch.umontreal.ca/cgi-bin/mfannot/mfannotInterface.pl. (Accessed: 28th January 2018)

64. P. Jones, D. Binns, H. Y. Chang, M. Fraser, W. Li, C. McAnulla, H. McWilliam, J. Maslen, A. Mitchell, G. Nuka, S. Pesseat, A. F. Quinn, A. Sangrador-Vegas, M. Scheremetjew, S. Y. Yong, R. Lopez, S. Hunter, InterProScan 5: genome-scale protein function classification. *Bioinformatics* **30**, 1236-1240 (2014).

65. T. M. Lowe, P. P. Chan, tRNAscan-SE On-Line: Integrating Search and Context for Analysis of Transfer RNA Genes. *Nucleic Acids Res,* **44**, W54–W57 (2016).

66. T. M. Lowe, S. R. Eddy, tRNAscan-SE: a program for improved detection of transfer RNA genes in genomic sequence. *Nucleic Acids Res* **25**, 955-964 (1997).

67. P. Danecek, A. Auton, G. Abecasis, C. A. Albers, E. Banks, M. A. DePristo, R. E. Handsaker, G. Lunter, G. T. Marth, S. T. Sherry, The variant call format and VCFtools. *Bioinformatics* **27**, 2156-2158 (2011).

68. D. J. Lawson, G. Hellenthal, S. Myers, D. Falush, Inference of population structure using dense haplotype data. *Plos Genet* **8**, e1002453 (2012).

69. O. Delaneau, B. Howie, A. J. Cox, J. F. Zagury, J. Marchini, Haplotype Estimation using sequencing reads. *Am J Hum Genet* **93**, 687-696 (2013).

70. D. Falush, M. Stephens, J. K. Pritchard, Inference of population structure using multilocus genotype data: Linked loci and correlated allele frequencies. *Genetics* **164**, 1567-1587 (2003).

71. G. Evanno, S. Regnaut, J. Goudet, Detecting the number of clusters of individuals using the software STRUCTURE: a simulation study. *Mol Ecol* **14**, 2611-2620 (2005).

72. X. Zheng, D. Levine, J. Shen, S. M. Gogarten, C. Laurie, B. S. Weir, A high-performance computing toolset for relatedness and principal component analysis of SNP data. *Bioinformatics* **28**, 3326-3328 (2012).

73. R Core Team. (R Foundation for Statistical Computing, Vienna, Austria, 2017).

74. H. Wickham, *ggplot2 : elegant graphics for data analysis*. Use R! (Springer, New York, 2009), pp. viii, 212 p.

75. K. L. Gosner, A simplified table for staging anuran embryos and larvae with notes on identification. *Herpetologica* **16**, 183-190 (1960).

76. D. G. Boyle, D. B. Boyle, V. Olsen, J. A. Morgan, A. D. Hyatt, Rapid quantitative detection of chytridiomycosis (*Batrachochytrium dendrobatidis*) in amphibian samples using real-time Taqman PCR assay. *Dis Aquat Organ* **60**, 141-148 (2004).

77. K. M. Kriger, H. B. Hines, A. D. Hyatt, D. G. Boyle, J. M. Hero, Techniques for detecting chytridiomycosis in wild frogs: comparing histology with real-time Taqman PCR. *Dis Aquat Organ* **71**, 141-148 (2006).

78. P. Kleinhenz, M. D. Boone, G. Fellers, Effects of the amphibian chytrid fungus and four insecticides on Pacific treefrogs (*Pseudacris regilla*). *J Herpetol* **46**, 625-631 (2012).

79. E. Luquet, T. W. Garner, J. P. Lena, C. Bruel, P. Joly, T. Lengagne, O. Grolet, S. Plenet, Genetic erosion in wild populations makes resistance to a pathogen more costly. *Evolution* **66**, 1942-1952 (2012).

80. M. J. Parris, T. O. Cornelius, Fungal pathogen causes competitive and developmental stress in larval amphibian communities. *Ecology* **85**, 3385-3395 (2004).

81. D. Darriba, G. L. Taboada, R. Doallo, D. Posada, ProtTest 3: fast selection of best-fit models of protein evolution. *Bioinformatics* **27**, 1164-1165 (2011).

82. K. Tamura, G. Stecher, D. Peterson, A. Filipski, S. Kumar, MEGA6: Molecular Evolutionary Genetics Analysis Version 6.0. *Mol Biol Evol* **30**, 2725-2729 (2013).

83. R. R. Wick, M. B. Schultz, J. Zobel, K. E. Holt, Bandage: interactive visualization of de novo genome assemblies. *Bioinformatics* **31**, 3350-3352 (2015).

84. M. J. Laforest, I. Roewer, B. F. Lang, Mitochondrial tRNAs in the lower fungus *Spizellomyces punctatus*: tRNA editing and UAG 'stop' codons recognized as leucine. *Nucleic Acids Res* **25**, 626-632 (1997).

85. E. Kayal, B. Bentlage, A. G. Collins, M. Kayal, S. Pirro, D. V. Lavrov, Evolution of linear mitochondrial genomes in medusozoan cnidarians. *Genome Biol Evol* **4**, 1-12 (2012).

86. Z. Shao, S. Graf, O. Y. Chaga, D. V. Lavrov, Mitochondrial genome of the moon jelly *Aurelia aurita* (Cnidaria, Scyphozoa): A linear DNA molecule encoding a putative DNA-dependent DNA polymerase. *Gene* **381**, 92-101 (2006).

87. M. Valach, Z. Farkas, D. Fricova, J. Kovac, B. Brejova, T. Vinar, I. Pfeiffer, J. Kucsera, L. Tomaska, B. F. Lang, J. Nosek, Evolution of linear chromosomes and multipartite genomes in yeast mitochondria. *Nucleic Acids Res* **39**, 4202-4219 (2011).

88. C. A. Brewer, http://www.ColorBrewer.org (2018).

89. E. Neuwirth, RColorBrewer: ColorBrewer Palettes. R package version 1.1-2. https://CRAN.R-project.org/package=RColorBrewer (2014).

90. M. Dowle, A. Srinivasan, data.table: Extension of `data.frame`. R package version 1.10.4. https://CRAN.R-project.org/package=data.table (2017).

91. G. Yu, D. Smith, H. Zhu, Y. Guan, T. T-Y. Lam, ggtree: an R package for visualization and annotation of phylogenetic trees with their covariates and other associated data. *Meth Ecol Evol* **8**, 28-36 (2017).

92. T. Galili, dendextend: an R package for visualizing, adjusting, and comparing trees of hierarchical clustering. *Bioinformatics* **31**, 3718-3720 (2015).

Acknowledgments:

DNA sequencing was carried out in the NBAF GenePool genomics facility at the University of Edinburgh, and we thank the GenePool staff for their assistance. This work used the computing resources of the UK MEDical BIOinformatics partnership - aggregation, integration, visualisation and analysis of large, complex data (UK MED-BIO) which is supported by the Medical Research Council [grant number MR/L01632X/1]. We thank Dr Johanna Rhodes for the provision of flow cells and reagents for MinION sequencing. We thank the staff at Oxford Nanopore Technologies for admission to the MinION Early Access Programme. We thank the three anonymous reviewers for constructive comments and suggestions during the peer review process.

Funding: SOH, TWJG, LB (Brookes), AL, AAC, DSS, EC, CM, JB, DA, FC and MCF were supported through NERC (standard grant NE/K014455/1). SOH acknowledges a Microsoft

563 Azure for Research Sponsorship (subscription ID: ab7cd695-49cf-4a83-910a-ef71603e708b).
564 TWJG, AL, AAC, DSS, EC, CM, JB, DA, FC and MCF were also supported by the EU
565 BiodivERsA scheme (R.A.C.E., funded through NERC directed grant NE/ G002193/1 and
566 ANR-08-Biodiversa-002-03) and NERC (standard grant NE/K012509/1). MCF, EC and CM
567 acknowledge the Nouragues Travel Grant Program 2014. RAF was supported by an MIT /
568 Wellcome Trust Fellowship. TWJG was supported by the People's Trust for Endangered
569 Species, the Morris Animal Foundation (D12ZO-002). JS and MCF were supported by the
570 Leverhulme Trust (RPG-2014-273) and the Morris Animal Foundation (D16ZO-022). FB
571 was supported by the ERC (grant ERC 260801 – Big_Idea). DMA was funded by Wellcome
572 Trust Grant 099202. JV was supported by the Hungarian Scientific Research Fund (OTKA
573 K77841) and Bolyai János Research Scholarship, Hungarian Academy of Sciences
574 (BO/00579/14/8). DG was supported by the Conservation Leadership Programme (grant
575 0134010) with additional assistance from F. Gebresenbet, R. Kassahun and S.P. Loader. CS-
576 A was supported by Fondecyt Nº11140902 and 1181758. TD-B was supported by the Royal
577 Geographical Society and the Royal Zoological Society of Scotland with assistance from
578 Mareike Hirschfeld and the Budongo Conservation Field Station. BW was supported by the
579 National Research Foundation of Korea (2015R1D1A1A01057282). LFT was supported by
580 FAPESP (#2016/25358-3) and CNPq (#300896/2016-6). LB (Berger), LFS and RJW were
581 supported by the Australian Research Council (FT100100375, DP120100811). AAC was
582 supported by a Royal Society Wolfson Research Merit award. JH, AL and SM were funded
583 by the Swedish Research Council Formas (grant no. 2013-1389-26445-20). CW was funded
584 by the National Research Foundation, South Africa. TYJ and TSJ acknowledge a National
585 Science Foundation Grant (DEB-1601259). WEH was funded by the NSERC Strategic and
586 Discovery grant programs.
587

Author contributions: All authors contributed ideas, data and editorial advice. S.J.O., A.R., R.C.F., K.A.M., B.B., and M.C.F. conducted analyses. G.M.R., T.W.J.G and L.B. conducted disease experiments. S.J.O., F.B., T.W.J.G. and M.C.F. wrote the paper with input from all authors.

Competing interests: KAM sits on an expert panel at the European Food Safety Authority addressing the risks of importation and spread of the salamander chytrid *Batrachochytrium salamandrivorans*, a species of fungus that is the closest known relative to the pathogen addressed in this manuscript.

Data availability: Sequences have been deposited in the National Center for Biotechnology Information (NCBI) Sequence Read Archive (SRA). All sequences are available from NCBI BioProject accession PRJNA413876 (https://www.ncbi.nlm.nih.gov/bioproject/PRJNA413876). The supplementary materials contain additional data. Phylogenetic trees are available from TreeBASE, project accession url: http://purl.org/phylo/treebase/phylows/study/TB2:S22286. A browsable version of the phylogeny and metadata in Fig. 1B is accessible at: https://microreact.org/project/GlobalBd

List of supplementary materials:

Materials and Methods

Figs. S1 to S15

Tables S1 to S5

Data S1 to S3

References (45-92)

Tables:

Lineage	Number of Isolates	Total segregating sites	Average pairwise-segregating sites	Total homozygous segregating sites	Average pairwise-homozygous segregating sites	π	Tajima's *D*
*Bd*ASIA-1	8	327,996	142,437	108,353	21,716	0.0044	0.2540
*Bd*ASIA-2 / *Bd*BRAZIL	12	148,021	51,069	48,722	6,216	0.0018	0.9825
*Bd*CAPE	24	146,466	38,881	53,884	4,977	0.0016	0.3143
*Bd*GPL	187	127,770	26,546	68,493	3,101	0.0009	0.9792

Table 1. Comparison of common genetic diversity measures among *Batrachochytrium dendrobatidis* lineages. Total segregating sites for each lineage include all segregating sites where genotype calls were made in at least half of the isolates. Average pairwise-segregating sites is the average number of sites with different genotypes between all pairs of isolates within a lineage. Total homozygous segregating sites includes all sites within a lineage where there is at least one homozygous difference between isolates. Average pairwise homozygous segregating sites is the average number of sites with different homozygous genotypes between all pairs of isolates within a lineage. Nucleotide diversity (π) is the mean of the per-site nucleotide diversity. Tajima's *D* is reported as the mean over 1 kbp bins.

Figures:

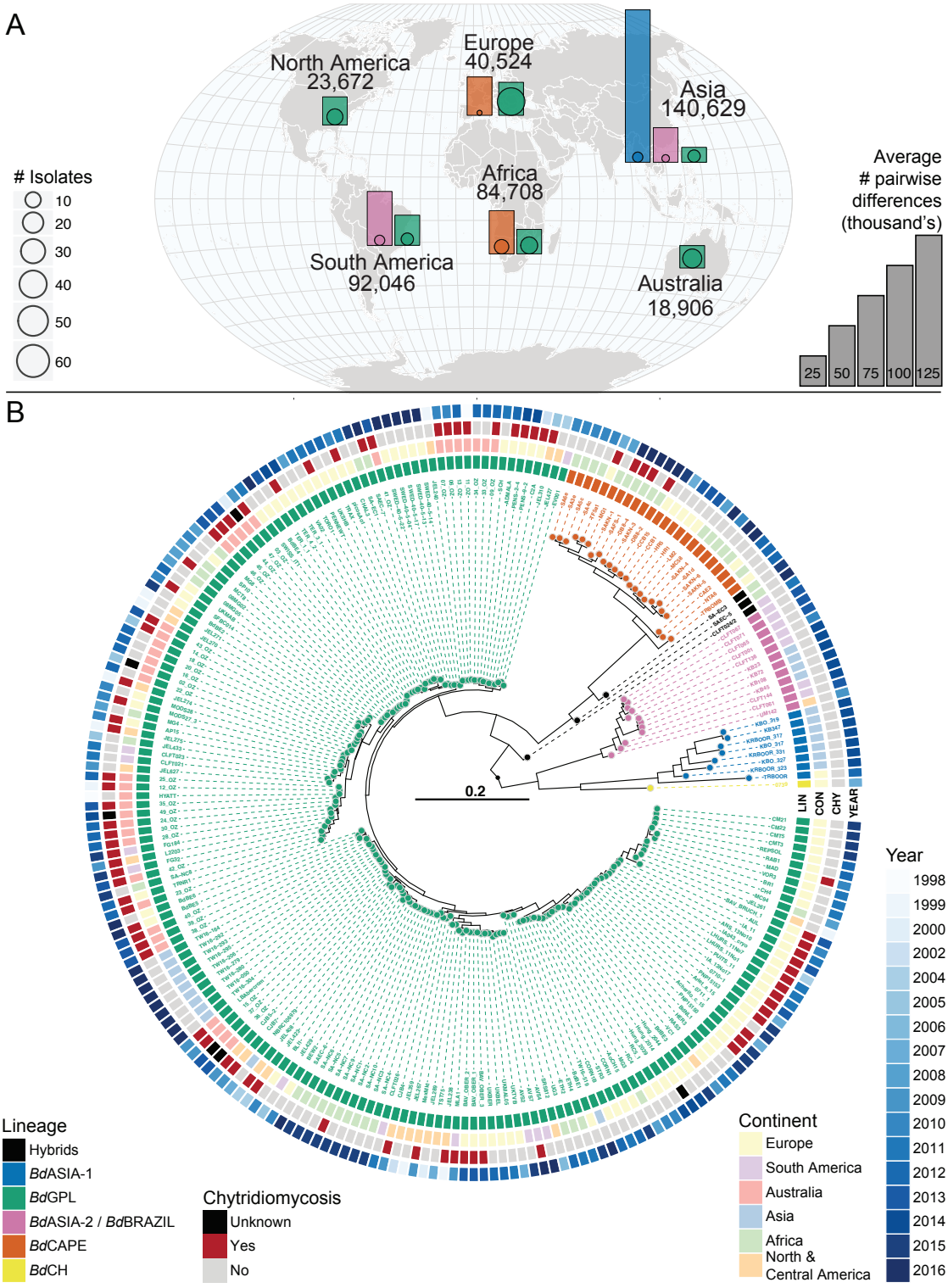

Fig. 1: Genetic diversity and phylogenetic tree of a global panel of 234 *Batrachochytrium dendrobatidis* isolates. **A.** Map overlaid with bar charts showing the relative diversity of isolates found in each continent and by each major lineage (excluding isolates from traded animals). The bar heights are the average number of segregating sites between all pairwise

combinations of isolates of each lineage in each continent (therefore only lineages with two or more isolates from a continent are shown). Outlined points at the base of each bar are scaled by the number of isolates for each lineage in that continent. The numbers around the outside of the globe are the average number of segregating sites between all pairwise combinations of isolates grouped by continent. Colours denote lineage as given by the legend in Fig 1B. **B.** Midpoint rooted radial phylogeny supports four deeply diverged lineages of *B. dendrobatidis*: *Bd*ASIA-1; *Bd*ASIA-2/*Bd*BRAZIL; *Bd*CAPE and *Bd*GPL. All major splits within the phylogeny are supported by 100% of 500 bootstrap replicates. See Fig. S2 for tree with full bootstrap support values on all internal branches.

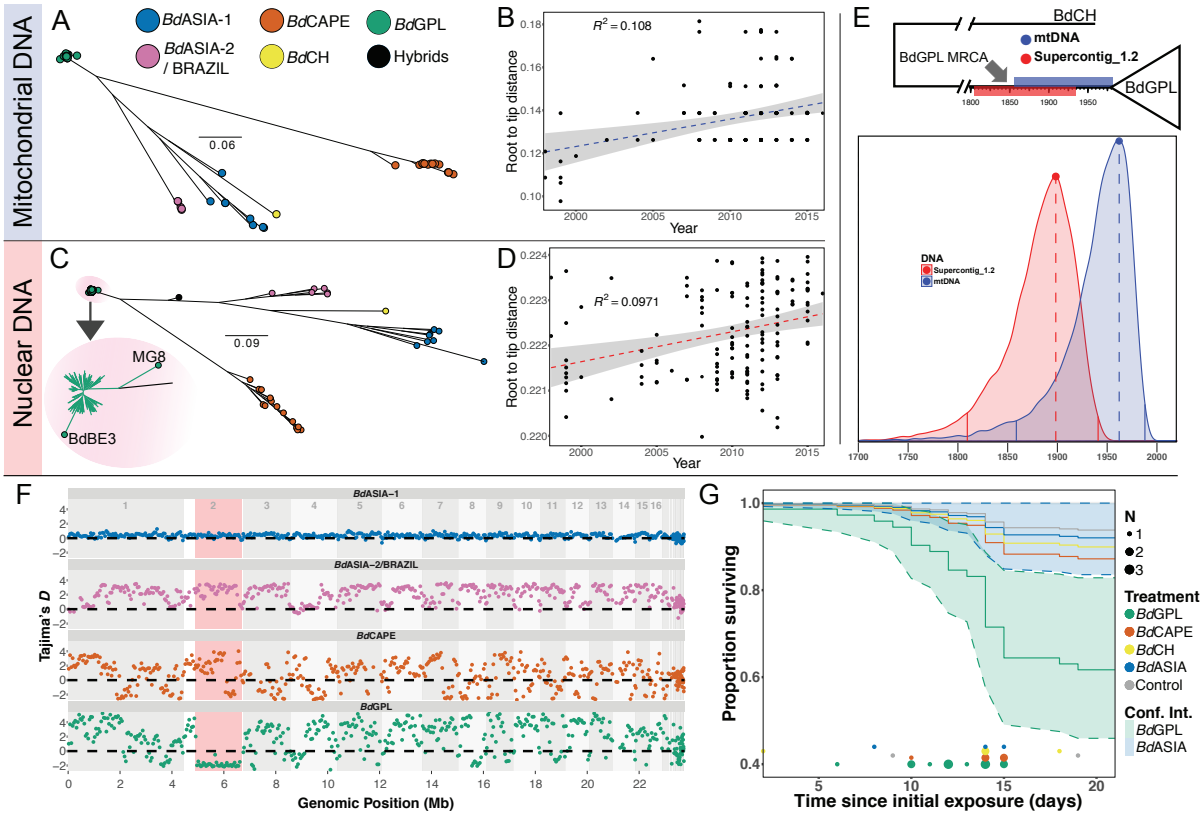

640

641 **Fig. 2:** Dating the emergence of *Bd*GPL. **A.** Maximum likelihood (ML) tree constructed from
642 1,150 high quality SNPs found within the 178 kbp mitochondrial genome. **B**. Linear
643 regression of root-to-tip distance against year of isolation for *Bd*GPL isolates in
644 mitochondrial DNA phylogeny in panel A, showing significant temporal trend (F-statistic =
645 14.35, p = 0.00024). **C.** ML tree constructed from a 1.66 Mbp region of low recombination in
646 Supercontig_1.2. Two *Bd*GPL isolates, BdBE3 and MG8 fall on long branches away from
647 the rest of the *Bd*GPL isolates (see inset zoom), due to introgression from another lineage
648 (*Bd*CAPE; see Fig. 3B) and were excluded from the dating analysis. **D.** Linear regression of
649 root-to-tip distance against year of isolation for *Bd*GPL isolates from phylogeny in panel C,
650 with significant temporal trend (F-statistic = 15.92, p-value = 0.0001). **E.** Top figure shows
651 *Bd*GPL and outgroup *Bd*CH, with the 95% HPD estimates for MRCA for *Bd*GPL from
652 mtDNA dating (blue) and nuclear DNA dating (red). Lower figure shows full posterior
653 distributions from tip dating models for mtDNA (blue) and partial nuclear DNA (red)
654 genomes. Solid vertical lines are limits of the 95% HPD. Dashed vertical lines denote the
655 maximal density of the posterior distributions. **F.** Sliding 10 kb, non-overlapping window
656 estimates of Tajima's D for each of the main *B. dendrobatidis* lineages. The region
657 highlighted in red is the low recombination segment of Supercontig_1.2. **G.** Survival curves
658 for *Bufo bufo* metamorphs for different *B. dendrobatidis* treatment groups: *Bd*ASIA-1 (blue);
659 *Bd*CAPE (orange); *Bd*CH (yellow); *Bd*GPL (green) and Control (grey). Confidence intervals

660 are shown for *Bd*GPL and *Bd*ASIA-1, showing no overlap by the end of the experiment.
661 Instances of mortalities in each treatment group are plotted along the x-axis, with points
662 scaled by number of mortalities at each interval (day).
663
664

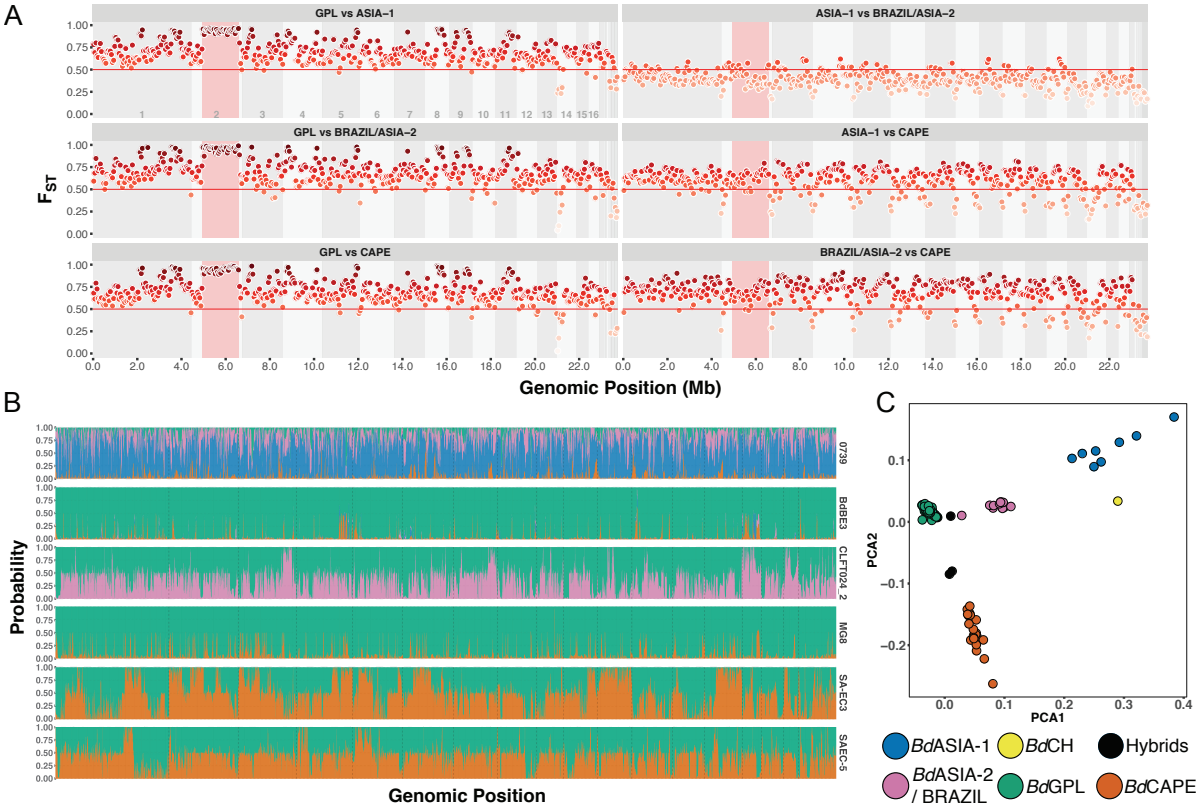

Fig. 3: F_{ST} and site-by-site STRUCTURE analysis. **A.** Non-overlapping, 10 kb sliding window of F_{ST} between lineages. The region highlighted in red is Supercontig_1.2:500,000-2,160,000 low recombination region. **B.** Site-by-site analysis of population ancestry for a random selection of 9,905 SNPs. Results show those isolates found to be either hybrid (SA-EC3, SA-EC5 and CLFT024/2), or with significant introgression from non-parental lineages (isolates BdBE3 and MG8) or a chimera of un-sampled diversity, likely originating from East Asia (0739, the *Bd*CH isolate). Each column represents a bi-allelic SNP position. The column is coloured according to the joint-probability of either allele copy arising from one of four distinct populations. Colours represent assumed parental lineages as given in Fig. 3C**. C.** Principle Components Analysis (PCA) of 3,900 SNPs in linkage equilibrium. Each point represents an isolate, coloured by phylogenetic lineage. The isolates separate into clearly defined clusters. The axes plot the first and second principle components.

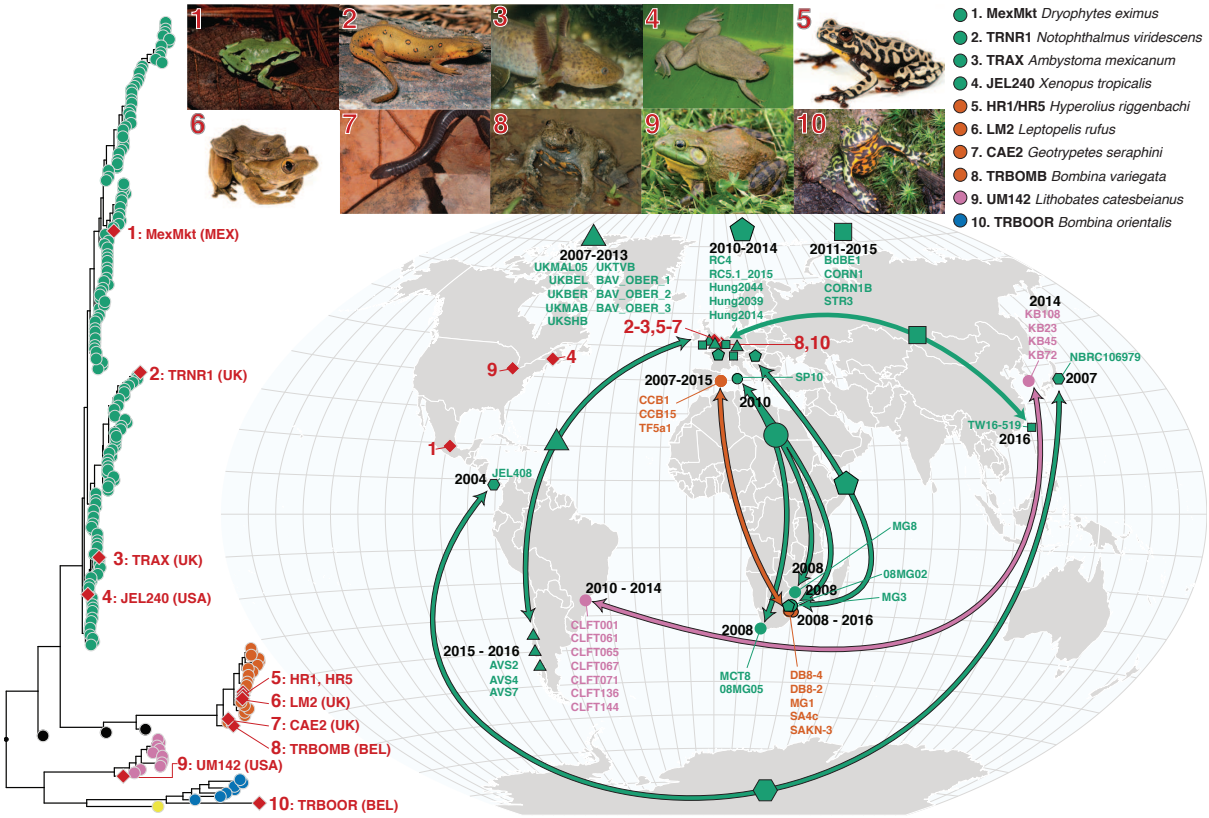

Fig. 4: Genotypes of *Bd* isolated from infected amphibians in the international trade and phylogenetically linked genotypes from segregated geographic localities. The red diamonds on the phylogeny indicate isolates recovered from traded animals. Their geographic location is displayed by the red diamonds on the map. The red numbers link each trade isolate to the relevant picture of the donor host species atop the figure panel and their placement in the phylogeny. The arrows on the map link geographically separated isolates which form closely related phylogenetic clades with high bootstrap support (≥90%). Each clade is denoted by a different shape point on the map with the names of isolates within each clade displayed on the map. The dates displayed indicate the sampling time-frame for each clade. The phylogenetic position of each clade is displayed in Figs S10-14. The colours of points and arrows on the map indicate lineage according to the legend in Fig 1. A browsable version of this phylogeny can be accessed at https://microreact.org/project/GlobalBd. Photo credits: (1) *Hyla eximia* Ricardo Chaparro, *(2) Notophthalmus viridescens* Patrick Coin / CC-BY-SA 2.5, *(3) Ambystoma mexicanum* Henk Wallays, *(4) Xenopus tropicalis* Daniel Portik, *(5) Hyperolis riggenbachi* and (6) *Leptopelis rufus* Brian Freiermuth, *(7) Geotrypetes seraphini* Peter Janzen, (8) *Bombina variegata* and (9) *Rana catesbeiana* and (10) *Bombina orientalis* Frank Pasmans